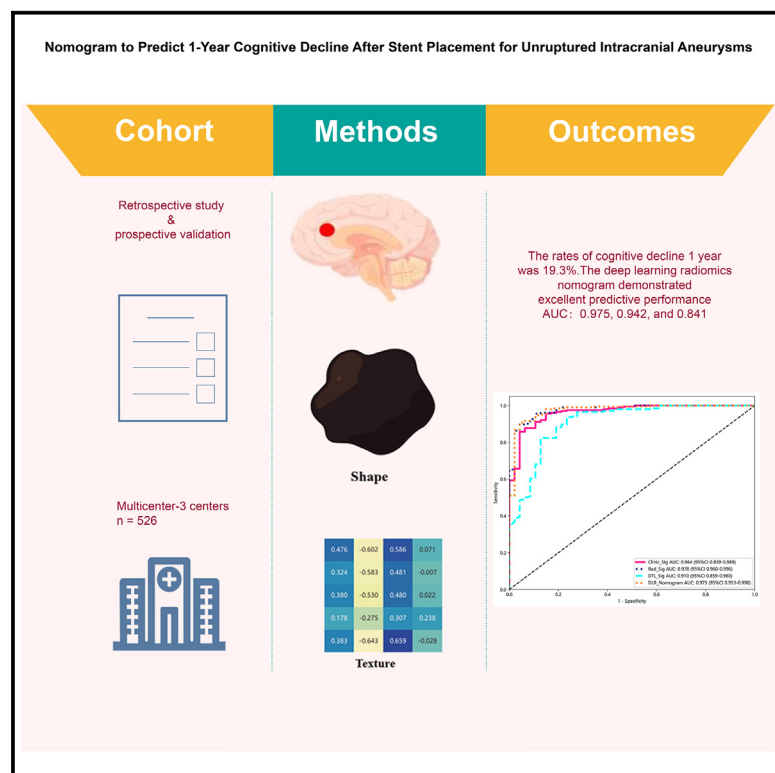


# Nomogram to predict 1-year cognitive decline after stent placement for unruptured intracranial aneurysms

## Graphical abstract



## Authors

Wenqiang Li, Chao Wang, Yuzhao Lu, ..., Jian Liu, David M. Hasan, Yang Wang

## Correspondence

wangyang7839@163.com

## In brief

Clinical neuroscience; Neurology

## Highlights

- NICIs linked to 19.4% cognitive decline at 1-year follow-up in UIA patients
- Nomogram combines NICI radiomics, DWI features, and clinical factors effectively
- High accuracy achieved with AUC of 0.975, 0.942, and 0.841 in validation cohorts
- Nomogram predicts cognitive outcomes post-stent placement in UIA patients



## Article

# Nomogram to predict 1-year cognitive decline after stent placement for unruptured intracranial aneurysms

Wenqiang Li,<sup>1,2,9</sup> Chao Wang,<sup>1,2,9</sup> Yuzhao Lu,<sup>3,9</sup> Junfan Chen,<sup>4,9</sup> Wenbin Li,<sup>5</sup> Yunpeng Liu,<sup>6</sup> Ziqing Zhang,<sup>6</sup> Zeping Jin,<sup>6</sup> Yiqi Liu,<sup>6</sup> Song Tan,<sup>3</sup> Zhiwei Zhang,<sup>7</sup> Xiaofei Huang,<sup>3</sup> Cong Ding,<sup>3</sup> Linfeng Zhang,<sup>3</sup> Jian Liu,<sup>1,2,10,11</sup> David M. Hasan,<sup>8,10,11</sup> and Yang Wang<sup>3,6,10,12,\*</sup>

<sup>1</sup>Department of Interventional Neuroradiology, Beijing Neurosurgical Institute, Capital Medical University, Beijing, China

<sup>2</sup>Department of Neurosurgery, Beijing Tiantan Hospital, Capital Medical University, Beijing, China

<sup>3</sup>Department of Neurosurgery, The First Affiliated Hospital of Nanchang University, Nanchang University, Nanchang, China

<sup>4</sup>Department of Interventional Neuroradiology, The First Affiliated Hospital of Zhengzhou University, Zhengzhou University, Zhengzhou, China

<sup>5</sup>Department of Magnetic Resonance Imaging, The First Affiliated Hospital of Zhengzhou University, Zhengzhou University, Zhengzhou, China

<sup>6</sup>Department of Neurosurgery, Beijing Chaoyang Hospital, Capital Medical University, Beijing, China

<sup>7</sup>SingularityFlow Co. Ltd., Beijing, China

<sup>8</sup>Department of Neurosurgery, Duke University, Durham, NC, USA

<sup>9</sup>These authors contributed equally

<sup>10</sup>These authors contributed equally

<sup>11</sup>Senior authors

<sup>12</sup>Lead contact

\*Correspondence: [wangyang7839@163.com](mailto:wangyang7839@163.com)

<https://doi.org/10.1016/j.isci.2025.111839>

## SUMMARY

New iatrogenic cerebral infarcts (NICIs) are common findings on diffusion-weighted magnetic resonance imaging (DWI) following stent placement for unruptured intracranial aneurysms (UIAs) and may contribute to cognitive decline (CD). Using posttreatment DWI and clinical features, we developed a deep learning radiomics nomogram (DLRN) to predict 1-year CD in NICI patients. In a multicenter cohort of 526 patients, CD rates at 1 year were 18.7% (47/251) in the training cohort, 19.8% (33/167) in the external validation cohort, and 20.4% (22/108) in the prospective cohort. The DLRN achieved excellent predictive performance with areas under the curve of 0.975, 0.942, and 0.841 for the respective cohorts. Calibration and decision curve analyses confirmed its reliability and clinical utility. This tool could facilitate early identification of high-risk patients, enabling timely, and tailored interventions to protect cognitive function.

## INTRODUCTION

Endovascular treatment of unruptured intracranial aneurysms (UIAs) has gained widespread acceptance. With advancements in stent design and technology, more UIA patients are being treated with stent implantation.<sup>1,2</sup> Small new iatrogenic cerebral infarcts (NICIs) may occur as a complication of endovascular procedures and are often detected using diffusion-weighted magnetic resonance imaging (DWI). Reported incidence rates range from 51% to 64%.<sup>3,4</sup> Although most NICIs are asymptomatic, some result in neuronal necrosis.<sup>5</sup>

Silent brain infarcts have been linked to cognitive decline (CD) in several studies.<sup>6–8</sup> However, the patients in these studies had small vessel cerebrovascular disease or cardiovascular disease, which differ mechanistically from iatrogenic cerebral infarction. The NeuroVISION study reported that perioperative covert stroke is associated with an increased risk of cognitive decline 1-year after non-cardiac surgery.<sup>9</sup> Many studies of patients with UIAs have found that NICIs related to endovascular treatment do not

affect cognitive function.<sup>10–13</sup> However, these studies are limited by factors including their small sample size and lack of confirmatory evidence of NICIs based on brain MRI. Recently, Ganesh et al. conducted a study in UIA patients who underwent endovascular treatment and reported that NICIs were associated with subtle differences in postprocedural and 30-day cognitive function outcomes; moreover, earlier dysfunction correlated with later differences.<sup>5</sup> However, it is still unclear whether NICIs are associated with cognitive function at later time periods.

Radiomics extracts numerous quantitative features from medical imaging and integrates key features into an image-based biomarker.<sup>14,15</sup> Many studies have emphasized the value of radiomics for diagnosing ischemic stroke and predicting clinical outcomes.<sup>16–18</sup> Liu et al.<sup>19</sup> reported that brain MRI radiomics can accurately diagnose subcortical ischemic vascular cognitive impairment. Furthermore, the incorporation of deep learning enables radiomics to capture intricate structures associated with particular tasks, resulting in outstanding clinical outcome prediction performance.<sup>20–22</sup>



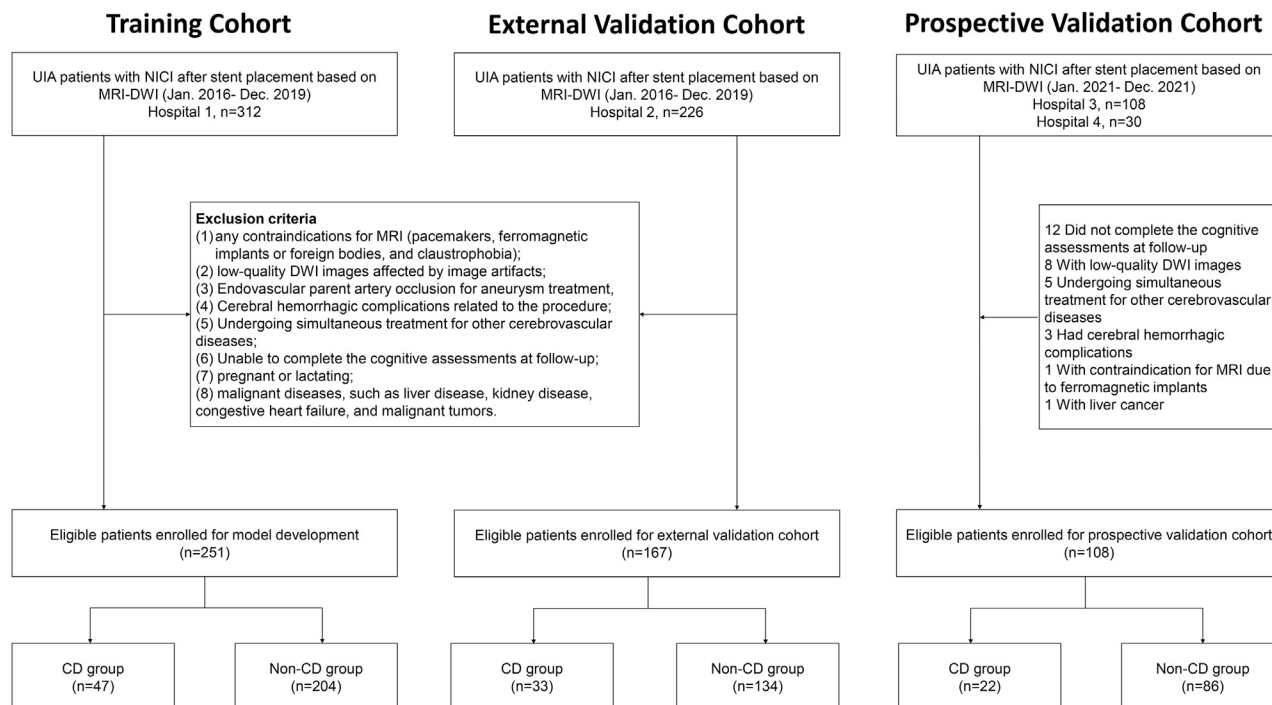


Figure 1. Flow diagram of the study

We hypothesized that UIA patients with NICIs after stent placement have CD at the 1-year follow-up and that brain MRI radiomics and deep learning features provide valuable information for predicting CD. In this study, we aimed to develop a model combining NICI radiomics, deep learning features derived from postoperative DWI, and clinical factors for the prediction of 1-year cognitive function outcomes. An integrated nomogram combining radiomics, deep learning data, and clinical factors was also constructed. The predictive performance of the signature and nomogram was tested on external retrospective and prospective validation cohorts.

## RESULTS

### Patient characteristics and outcome

In total, 418 patients were included in the retrospective studies: 251 in the training cohort and 167 in the external validation cohort (Figure 1). The prospective external validation study enrolled 138 patients between January 2021 and December 2021; after excluding 30 (21.7%) based on criteria, 108 were included for analysis (Figure 1). Patient characteristics in the three cohorts are shown in Table 1. In the training cohort, 18.7% (47/251) of patients had cognitive impairment at the 1-year follow-up, which was similar to the proportions in the external validation cohort (19.8%,  $p = 0.792$ ) and prospective validation cohort (20.4%;  $p = 0.717$ ).

### Clinical predictors

Comparisons of clinical characteristics between the CD and non-CD groups in the training, external validation, and prospective

validation cohorts are presented in Table S1. The number and volume of NICIs were significantly higher in the CD group in all three cohorts than in the non-CD group. Hypertension, history of ischemic stroke, and multiple stents were significantly more prevalent in the CD group in the training and external validation cohorts. The procedure time was significantly longer in the CD group in the training and prospective validation cohorts. The prevalence of diabetes was significantly higher in the CD group in the training cohort. In the external validation cohort, preoperative modified Rankin scale score and blood glucose level were significantly higher in the CD group. A history of hemorrhagic stroke was significantly more prevalent in the CD group in the prospective validation cohort. The integrated clinical signature identified the clinical factors in the training cohort (including number and volume of NICIs, procedure time, diabetes, hypertension, history of ischemic stroke, and multiple stents) as significant predictors of CD at the 1-year follow-up. Among these, the number and volume of NICIs and procedure time were most important (Figure S1). And no significant difference was observed in age and gender in each cohort. No obvious linear relationship (correlation coefficient  $>0.9$ ) was observed between these significant clinical features (Figure S2).

### Radiomic signature building

Using LASSO penalization methods, parameters were set to  $\lambda$  of 0.022 for the radiomics signature (Figure S3). Fifteen radiomics features were shown to be predictive of CD at the 1-year follow-up. Definitions of the radiomics features are shown in Table S2. None of the features with a correlation coefficient  $>0.9$  between any two features was excluded (Figure S4). The

**Table 1. Patient characteristics in the three study cohorts**

Characteristics	Training cohort (N = 251)	External validation cohort (N = 167)	Prospective validation cohort (N = 108)	P <sup>a</sup>	P <sup>b</sup>	P <sup>c</sup>
Age, y	56.12 ± 10.32	60.95 ± 9.53	56.00 ± 10.40	<0.001	0.960	<0.001
Female	166 (66.14)	120 (71.86)	72 (66.67)	0.261	1	0.435
Symptom	154 (61.35)	51 (30.54)	80 (74.07)	<0.001	0.027	<0.001
Pre_mRS	0.62 ± 0.58	0.13 ± 0.37	0.76 ± 0.45	<0.001	0.009	<0.001
Smoking history	53 (21.12)	28 (16.77)	19 (17.59)	<0.001	0.535	<0.001
Education, y	10.39 ± 2.87	9.17 ± 2.67	8.94 ± 2.86	<0.001	<0.001	0.498
<b>Comorbidities</b>						
Diabetes	33(13.15)	18(10.78)	8(7.41)	0.567	0.165	0.470
Hypertension	114(45.42)	79(47.31)	60(55.56)	0.780	0.099	0.225
Ischemic stroke	58(23.11)	17(10.18)	22(20.37)	0.001	0.665	0.029
Hemorrhagic stroke	2(0.80)	7(4.19)	13(12.04)	0.046	<0.001	0.027
CAD	8(3.19)	1(0.60)	5(4.63)	0.149	0.717	0.070
Hyperlipidemia	108(43.03)	57(34.13)	8(7.41)	0.068	<0.001	<0.001
<b>Concomitant medication</b>						
Statin	120(47.81)	67(40.12)	8(7.41)	0.121	<0.001	<0.001
DAPT, days	4.09 ± 1.41	3.83 ± 1.89	6.31 ± 2.38	0.314	<0.001	<0.001
<b>Aneurysm data</b>						
Maximum size	7.58 ± 5.59	6.10 ± 4.05	7.76 ± 5.38	0.064	0.422	0.007
Neck size	5.16 ± 3.53	4.19 ± 1.99	5.24 ± 3.04	0.066	0.192	0.002
PA diameter	3.68 ± 0.62	3.07 ± 1.00	3.54 ± 0.98	<0.001	0.005	<0.001
Size ratio	2.10 ± 1.55	2.17 ± 1.44	1.46 ± 0.37	0.119	0.06	<0.001
Aspect ratio	1.45 ± 0.49	1.43 ± 0.70	1.47 ± 0.72	0.327	0.355	0.961
<b>Procedural data</b>						
Procedure time	2.09 ± 0.92	2.38 ± 1.01	1.45 ± 0.66	<0.001	<0.001	<0.001
Flow diverter	116(46.22)	45(26.95)	47(43.52)	<0.001	0.639	0.004
Overlapping stents	15(5.98)	6(3.59)	4(3.70)	0.275	0.378	0.962
Stent length	20.55 ± 6.10	23.03 ± 6.01	21.25 ± 6.53	<0.001	0.351	<0.001
<b>Laboratory data</b>						
WBC, /μL	6.20 ± 1.79	5.82 ± 1.73	5.91 ± 1.61	0.016	0.161	0.456
RBC, ×10 <sup>6</sup> /μL	4.43 ± 0.47	4.36 ± 0.70	4.34 ± 0.41	0.011	0.045	0.680
HL, g/dL	137.12 ± 15.40	127.10 ± 14.73	133.47 ± 13.21	<0.001	0.032	<0.001
Platelet count	230.02 ± 53.81	221.98 ± 56.63	229.45 ± 55.10	0.153	0.743	0.372
Hematocrit	39.96 ± 3.95	1.29 ± 5.75	39.59 ± 3.74	<0.001	0.417	<0.001
PT	10.88 ± 0.93	11.12 ± 0.96	10.67 ± 0.75	0.088	0.009	<0.001
APTT	30.48 ± 3.90	27.81 ± 4.36	29.04 ± 3.10	<0.001	<0.001	<0.001
INR	1.00 ± 0.07	0.93 ± 0.07	0.96 ± 0.07	<0.001	<0.001	0.001
Blood glucose	5.31 ± 1.19	5.46 ± 1.30	5.10 ± 1.48	0.219	0.012	<0.001
TG	1.90 ± 2.72	1.65 ± 1.14	1.56 ± 0.85	0.651	0.479	0.770
TC	4.45 ± 1.14	4.49 ± 0.99	4.19 ± 0.96	0.349	0.139	0.016
LDL	2.73 ± 0.90	2.67 ± 0.74	2.44 ± 0.86	0.751	0.012	0.020
HDL	1.27 ± 0.42	1.34 ± 0.47	1.29 ± 0.47	0.068	0.744	0.243
<b>Radiologic findings</b>						
Location of NICI (AC)	214 (85.3)	162 (97.0)	104 (96.3)	<0.001	0.747	0.003

(Continued on next page)

Table 1. Continued

Characteristics	Training cohort (N = 251)	External validation cohort (N = 167)	Prospective validation cohort (N = 108)	P <sup>a</sup>	P <sup>b</sup>	P <sup>c</sup>
Number of NICI	13.50 ± 17.23	10.96 ± 10.70	7.54 ± 7.93	0.094	<0.001	0.005
Volume of NICI	157.11 ± 310.49	191.70 ± 438.73	541.73 ± 345.03	0.346	<0.001	<0.001

Pre-mRS, preoperative modified Rankin scale score; CAD, coronary artery disease; DAPT, dual antiplatelet therapy; PA, parent artery; WBC, white blood cell count; RBC, red blood cell count; HL, hemoglobin level; PT, prothrombin time; APTT, activated partial thromboplastin time; INR, international normalized ratio; TG, triglyceride; TC, total cholesterol; LDL-C, low-density lipoprotein cholesterol; HDL-C, high-density lipoprotein cholesterol; NICI, new iatrogenic cerebral infarction; AC, anterior circulation.

<sup>a</sup>Training vs. External validation.

<sup>b</sup>Training vs. Prospective validation.

<sup>c</sup>External validation vs. Prospective validation.

importance of the selected radiomics features is shown in [Figure S3](#). Across 5-fold cross verification, the LR machine learning model showed good interpretability and stable and good performance ([Figure S5](#)); this model was therefore selected for final radiomics signature model building. Calculation of the rad-score was performed using the formula shown in [Table S3](#).

### Deep transform learning signature building

The performances of six deep transform learning (DTL) models (Densenet121, densenet201, Inception v3, Resnet50, Resnet101, and Vgg19) are shown in [Table S4](#). Overall, the Resnet50 model achieved the best accuracy for predicting CD ([Table S4](#)). Although the Resnet101 model achieved the best area under the curve (AUC) of 0.940 (95% confidence interval [CI], 0.905–0.976) in the training cohort and the AUC of the Resnet50 model was 0.910 (95% CI, 0.859–0.960) in the training cohort, we still considered the external and prospective validation cohorts as the most important indicator. The AUC of the Resnet50 model was 0.902 (95% CI, 0.853–0.951) in the external validation cohort and 0.838 (95% CI, 0.727–0.948) in the prospective validation cohort. These values were superior to those of the other DTL models ([Table S4](#)). To investigate the interpretability of the DTL, we visualized the DTL model response areas for predicting CD by applying gradient-weighted class activation mapping ([Figure S6](#)). We found that the location of the strong response area may change. In most DWI images of patients without CD, the strong response areas frequently clustered on the edge of the infarction lesion. In contrast, the strong response areas usually clustered within the lesion in patients with CD. These results may explain the discrimination ability of the DTL to some extent.

### DLRN construction and performance comparison and evaluation

Multivariable binary logistic regression analysis was performed to build the deep learning radiomics nomogram (DLRN) from the clinical characteristics, radiomics, and DTL signatures ([Figure 2A](#)). Performance results are shown in [Table 2](#). Comparisons of model performance are presented in [Figure 2B](#).

In the external validation and prospective validation cohorts, DLRN showed superior performance in predicting CD compared with the conventional single-modality prediction models ([Figure 2B](#)). In the external validation cohort, DLRN achieved a favorable AUC (0.942 [95% CI, 0.896–0.987]), which was a 3.8% improvement over the clinical model (AUC, 0.908; 95% CI, 0.839–0.978),

3.2% improvement over the radiomic signature model (AUC, 0.910; 95% CI, 0.848–0.972), and 4.0% improvement over the DTL signature model (AUC, 0.902, 95% CI, 0.853–0.951; [Table 2](#)). These improvements were significant based on DeLong testing ([Table S5](#)). Similar results were seen in the prospective validation cohort: DLRN achieved a favorable AUC (0.841 [95% CI, 0.725–0.958]), which represented a 2.7% improvement in AUC over the clinical model (AUC, 0.814; 95% CI, 0.679–0.949), 7.6% improvement over the radiomic signature model (AUC, 0.765; 95% CI, 0.625–0.905), and 0.3% improvement over the DTL signature model (AUC, 0.838; 95% CI, 0.727–0.948; [Table 2](#)). With a threshold of 0.897, the DLRN score was significantly higher in the CD group than in the non-CD group in the training, external validation, and prospective cohorts (all  $p < 0.001$ ; [Figure S7](#)).

Accuracy for predicting CD was highest with the DLRN model ([Figure 2C](#)). With this model, the Hosmer-Lemeshow test was not significant in any of the training cohorts, demonstrating a good fit ([Table S6](#)). In the decision curve analysis, the AUC was higher with DLRN than with clinical signature, radiomics signature, and DTL signature ([Figure 2D](#)). In clinical practice, the DLRN demonstrated good diagnostic performance in distinguishing CD in both the external and prospective validation cohorts.

## DISCUSSION

In this multicenter study, we developed and validated a deep learning radiomics model based on DWI imaging to predict CD at 1-year follow-up in UIA patients with NICIs after stent placement. The DLRN showed high predictive ability and reproducibility across different centers, demonstrating the value of DWI-based deep learning radiomics in outcome prediction. Furthermore, combining radiomics extracted from MRI with clinical factors to construct a nomogram achieved better predictive value than models that used imaging data or clinical factors alone.

### CD in UIA patients with NICIs after endovascular treatment

Silent brain infarction has been linked to poor cognitive function and an increased risk of developing dementia.<sup>7,23</sup> New silent brain infarctions are frequently observed following cardiac and cerebrovascular endovascular procedures.<sup>3,8</sup> Substantial evidence from the cardiology literature has indicated that NICIs

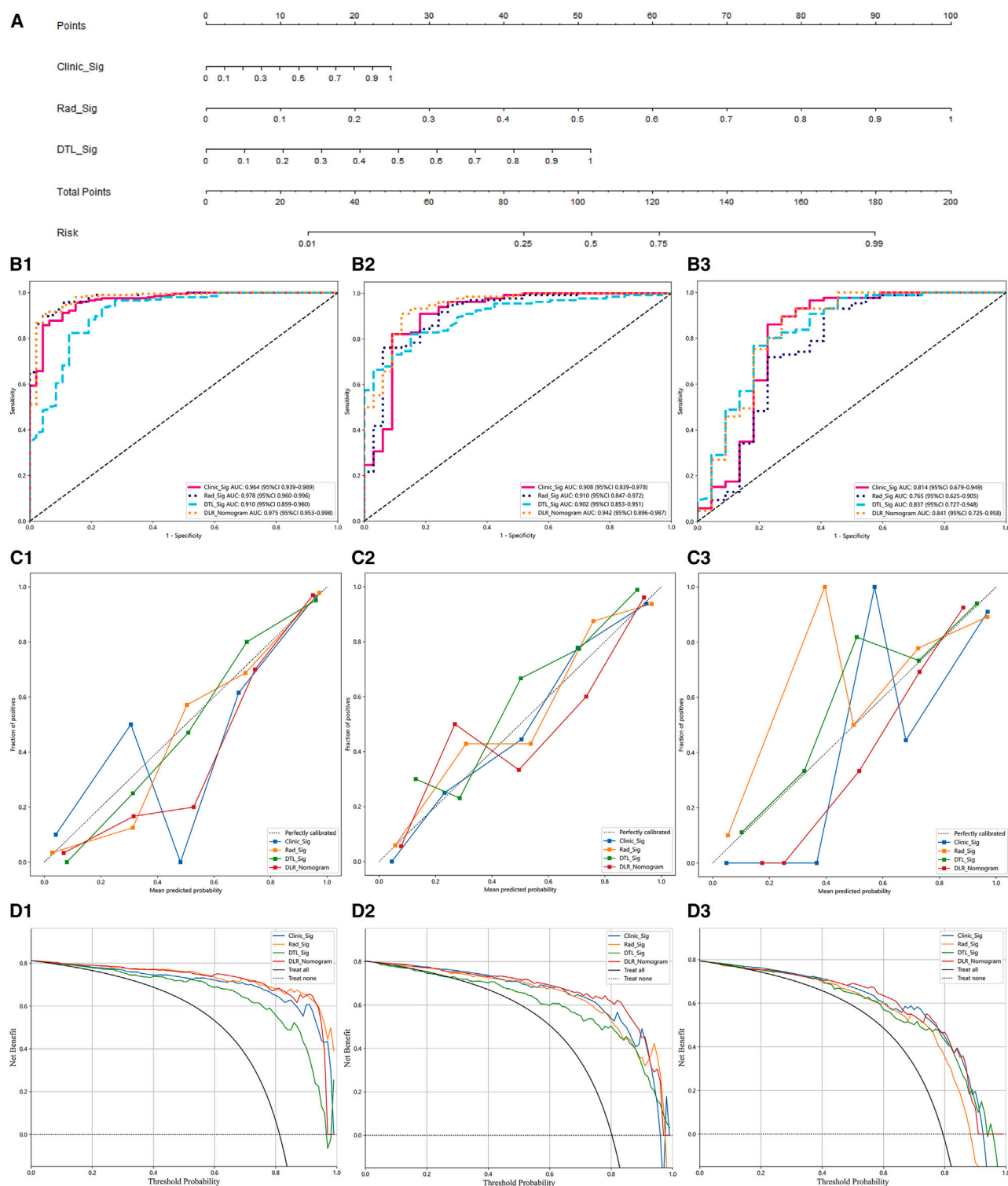


**Figure 2. The DLRN model was used to develop a nomogram which incorporated clinical features, radiomics signature, and DTL signature to predict cognitive decline**

(A) Comparison of the receiving operating characteristic curves of different models in the training cohort (B1), external validation cohort (B2), and prospective validation cohort (B3) The DLRN model demonstrated the best discriminating ability among these models. The area under the curve was 0.942

(legend continued on next page)



are frequently a precursor to symptomatic stroke and are associated with cognitive decline.<sup>8,24,25</sup> However, whether UIA patients with NICIs after endovascular treatment exhibit CD at 1-year follow-up is controversial.<sup>5,12</sup> The NeuroVISION study<sup>9</sup> reported that perioperative covert stroke is associated with an increased risk of CD 1 year after non-cardiac surgery. Ganesh et al.<sup>5</sup> also found that NICIs were associated with subtle differences in postprocedural and short-term cognitive function outcomes in UIA patients who underwent endovascular treatment. Nevertheless, the correlation between NICIs and 1-year CD after endovascular treatment of UIAs has not been clearly established. In our study, 18.7% of patients in the retrospective training cohort had cognitive impairment at the 1-year follow-up. Similar rates were found in the external validation and prospective cohorts (19.8% and 20.4%, respectively). The overall incidence of CD at the 1-year follow-up was 19.4%, which is much lower than the rate reported in the NeuroVISION study (42%). The primary reason for this difference may be related to the higher number of patients aged 65 years or older in the NeuroVISION study.

### **MULTIPLE FACTORS INFLUENCE COGNITIVE OUTCOMES**

Various risk factors that influence cognitive outcomes after endovascular treatment of cardiac disease have been documented. A direct correlation has been observed between the prevalence of diabetes and chronic renal disease and the mean number of new silent brain infarctions on post-procedural MRI, which further elevates the risk of cognitive decline. Moreover, additional factors also play a role, including thromboembolism, severe left ventricular dysfunction and heart failure, and procedure-specific factors (such as microemboli and hypoperfusion).<sup>8,26</sup> In neuroendovascular studies, several factors including age, female sex, large aneurysm size, antiplatelet therapy resistance, and total procedure time have been identified as risk factors for new DWI brain infarction lesions.<sup>27,28</sup> However, the number of studies is small and a correlation between NICIs and CD has not been established. Only one recent neuroendovascular study has examined NICIs and cognitive function; this study reported that cognitive outcomes were worse in patients with high infarct burden ( $\geq 10$  infarctions) than those who were infarct-free.<sup>5</sup>

Based on our study, the following features are listed in order of importance from highest to lowest: volume of NICIs, number of NICIs, procedure time, diabetes, hypertension, multiple stents, and history of ischemic stroke. These results are consistent with those of Ganesh et al.<sup>5</sup> Two of the most important factors contributing to CD are related to infarct burden (volume and number of NICIs), which are related to other factors. Diabetes, hypertension, and history of ischemic stroke might be independently linked to a higher risk of cerebrovascular disease. Procedure-related factors (procedure time and multiple stents) might be

associated with four potential mechanisms. Multiple stents may lead to in-stent thrombosis and vessel occlusion, distal thromboembolic events, thromboembolic events related to catheter and mechanical manipulation, and arterial branch occlusion.<sup>29</sup>

Radiomics research in stroke is accelerating rapidly. Radiomics has potential applications in almost every aspect of outcome prediction in patients with stroke.<sup>29,30</sup> However, few neuroimaging studies have explored imaging markers related to cognitive outcomes in patients with NICIs after endovascular treatment. Post-treatment DWI is the preferred imaging modality for the initial evaluation of cerebral infarction.<sup>3,5</sup> Previous studies reported that DWI radiomics can be used to prognosticate stroke outcomes; moreover, they have noted that integration of clinical factors and DWI radiomics provides more accurate long-term predictions.<sup>29</sup> However, the links between cognitive outcomes and DWI radiomic features in various types of cerebral infarction have not yet been revealed.

### **DLRN in predicting CD in UIA patients with NICIs after stent placement**

To the best of our knowledge, this is the first study to build and validate a clinical-radiomics nomogram that predicts 1-year cognitive outcomes of UIA patients with NICI after stent placement. From a methodological perspective, deep learning features have great potential to combine different imaging information for prognostication, as the acquired data are typically task-specific. Our nomogram combined clinical, radiomics, and deep learning features of NICIs, which improved the diagnostic performance for predicting 1-year CD in UIA patients with NICI after stent placement. This combined model also maintained its diagnostic performance in the retrospective and prospective validation sets. Accurate perioperative prediction of 1-year cognitive outcomes may assist clinicians in individualizing treatment plans to improve patient quality of life, as quality of life is closely related to selection of treatment, early warning, and early intervention. For example, Li et al.<sup>31</sup> reported that adjustment of antiplatelet therapy might reduce the high-risk radiomic features of UIA patients with high on-treatment platelet reactivity after stent placement. Moreover, the clinical risk factors influencing cognitive outcomes are modifiable; therefore, adjusting antiplatelet therapy and targeting these risk factors might reduce the incidence of CD in patients with NICIs after endovascular treatment. Furthermore, cognitive training may also improve or delay CD.<sup>32</sup>

### **Limitations of the study**

This study has several limitations. First, while the deep learning and radiomics model was validated using prospective data, the model itself was built on retrospective data. Additional prospective clinical trials would enhance its clinical applicability and reliability. Second, the patient cohort in this study was composed exclusively of individuals from China, necessitating further large-scale international validation to confirm the model's applicability to patients of diverse ethnicities and populations. Third,

---

in the external validation cohort and 0.841 in the prospective validation cohort. Calibration curves of different models for prediction of cognitive decline in the training cohort (C1), external validation cohort (C2), and prospective validation cohort (C3). Decision curve analysis demonstrated the clinical utility of the different models for predicting cognitive decline in the training cohort (D1), external validation cohort (D2), and prospective validation cohort (D3).

**Table 2. Prediction performance of the nomogram compared with the single-modality models**

	Training cohort	External validation cohort	Prospective validation cohort
<b>DLR Nomogram</b>			
ACC	0.916	0.904	0.860
AUC (95% CI)	0.975 (0.953–0.998)	0.942 (0.896–0.987)	0.841 (0.725–0.958)
SENS	0.907	0.910	0.894
SPEC	0.957	0.879	0.727
PPV	0.989	0.968	0.927
NPV	0.703	0.707	0.640
F1	0.946	0.938	0.910
<b>Clinical Signature</b>			
ACC	0.876	0.838	0.843
AUC (95% CI)	0.964 (0.939–0.989)	0.908 (0.839–0.978)	0.814 (0.679–0.949)
SENS	0.858	0.821	0.860
SPEC	0.957	0.909	0.773
PPV	0.989	0.973	0.937
NPV	0.608	0.556	0.586
F1	0.919	0.891	0.897
<b>Radiomic Signature</b>			
ACC	0.908	0.796	0.860
AUC (95% CI)	0.978 (0.960–0.996)	0.910 (0.848–0.972)	0.765 (0.625–0.905)
SENS	0.897	0.761	0.929
SPEC	0.957	0.939	0.591
PPV	0.989	0.981	0.898
NPV	0.682	0.492	0.684
F1	0.941	0.857	0.913
<b>DTL Signature</b>			
ACC	0.904	0.826	0.778
AUC (95% CI)	0.910 (0.859–0.960)	0.902 (0.853–0.951)	0.837 (0.727–0.948)
SENS	0.936	0.910	0.767
SPEC	0.766	0.879	0.818
PPV	0.946	0.968	0.943
NPV	0.735	0.707	0.474
F1	0.941	0.938	0.846

AUC, area under the receiver operating characteristic curve; CI, confidence interval; ACC, accuracy; SENS, sensitivity; SPEC, specificity; PPV, positive predictive value; NPV, negative predictive value.

the MRI scans were collected from four centers and utilized different imaging systems with varying acquisition parameters. Radiomics features are sensitive to these variations; hence, standardized DWI images were employed to normalize the image intensities after feature selection. Fourth, due to the retrospective design of the study, pre-treatment Mini-Mental State Examination (MMSE) scores were not recorded, and the MMSE itself has limited precision in assessing different subdivisions of cognitive functioning. This limitation may have led to underestimation,

as some patients with cognitive decline might not have been identified. Finally, lesion segmentation was performed manually by two neuroradiologists, which was time-consuming in this large study. Future research should focus on developing automatic volumetric segmentation algorithms to streamline the radiomics analysis process.

To conclude, we designed a nomogram based on deep learning DWI radiomics to predict CD at the 1-year follow-up in UIA patients with NICIs after stent placement. By combining DWI data and clinical factors, the DLRN provided high diagnostic accuracy. The proposed nomogram has considerable potential to enable individualized treatment of UIA patients with NICIs and potentially improve their management and cognitive outcomes.

## RESOURCE AVAILABILITY

### Lead contact

Further information and requests for resources should be directed to and will be fulfilled by the lead contact, Yang Wang ([wangyang7839@163.com](mailto:wangyang7839@163.com)).

### Materials availability

The study did not generate any new materials.

### Data and code availability

- All data generated during this study are available from the corresponding author on reasonable request. No new code was developed for this study.
- The data analyze methods used for this paper is available in Supplementary Text.
- The paper has been written in accordance with the Strengthening the Reporting of Observational Studies in checklist cross-sectional (STROBE).

## ACKNOWLEDGMENTS

We thank platform “One-key AI” for code consultation of this study. Fund: this work was supported by National Natural Science Foundation of China (grant numbers: 82201435 for Wenqiang Li, 82272092 for J.L. and 81960330 for Y.W.), China Postdoctoral Science Foundation (grant number: 2022M712893 for Wenqiang Li).

## AUTHOR CONTRIBUTIONS

Wenqiang Li performed the manuscript writing. Wenqiang Li, Yuzhao Lu, J.C., C.W., Yunpeng Liu, Ziqing Zhang, Z.J., Yiqi Liu, S.T., X.H., C.D., and L.Z. acquired the data. Wenqiang Li, Wenbin Li, Zhiwei Zhang, Y.W., and J.L. contributed to data analysis and interpretation. Wenqiang Li, Y.W., J.L., and D.M.H. contributed to the experimental design and manuscript revision, and handled funding and supervision.

## DECLARATION OF INTERESTS

All authors declare no competing interests.

## STAR★METHODS

Detailed methods are provided in the online version of this paper and include the following:

- **KEY RESOURCES TABLE**
- **EXPERIMENTAL MODEL AND STUDY PARTICIPANT DETAILS**
  - Ethical statement
  - Study population
  - Inclusion and exclusion criteria



- **METHOD DETAILS**
  - Experimental design
  - Data collection and cognitive evaluation
  - Image acquisition, segmentation, feature extraction, and selection
- **QUANTIFICATION AND STATISTICAL ANALYSIS**
  - Signature construction and assessment
  - Model validation and visualization

## SUPPLEMENTAL INFORMATION

Supplemental information can be found online at <https://doi.org/10.1016/j.isci.2025.111839>.

Received: May 22, 2024

Revised: October 9, 2024

Accepted: January 15, 2025

Published: January 17, 2025

## REFERENCES

1. Etminan, N., and Rinkel, G.J. (2016). Unruptured intracranial aneurysms: development, rupture and preventive management. *Nat. Rev. Neurol.* **12**, 699–713.
2. Walcott, B.P., Stapleton, C.J., Choudhri, O., and Patel, A.B. (2016). Flow Diversion for the Treatment of Intracranial Aneurysms. *JAMA Neurol.* **73**, 1002–1008.
3. Hahnenmann, M.L., Ringelstein, A., Sandalcioğlu, I.E., Goericke, S., Moeninghoff, C., Wanke, I., Forsting, M., Sure, U., and Schlamann, M. (2014). Silent embolism after stent-assisted coiling of cerebral aneurysms: diffusion-weighted MRI study of 75 cases. *J. Neurointerv. Surg.* **6**, 461–465.
4. Bond, K.M., Brinjikji, W., Murad, M.H., Kallmes, D.F., Cloft, H.J., and Lanzino, G. (2017). Diffusion-Weighted Imaging-Detected Ischemic Lesions following Endovascular Treatment of Cerebral Aneurysms: A Systematic Review and Meta-Analysis. *AJNR. Am. J. Neuroradiol.* **38**, 304–309.
5. Ganesh, A., Goyal, M., Wilson, A.T., Ospel, J.M., Demchuk, A.M., Mikulis, D., Poubanc, J., Krings, T., Anderson, R., Tymianski, M., et al. (2022). Association of Iatrogenic Infarcts With Clinical and Cognitive Outcomes in the Evaluating Neuroprotection in Aneurysm Coiling Therapy Trial. *Neurology* **98**, e1446–e1458.
6. Sigurdsson, S., Aspelund, T., Kjartansson, O., Gudmundsson, E.F., Jonsson, M.K., Eiriksdottir, G., Jonsson, P.V., van Buchem, M.A., Gudnason, V., and Launer, L.J. (2017). Incidence of Brain Infarcts, Cognitive Change, and Risk of Dementia in the General Population: The AGES-Reykjavik Study (Age Gene/Environment Susceptibility-Reykjavik Study). *Stroke* **48**, 2353–2360.
7. Vermeer, S.E., Prins, N.D., den Heijer, T., Hofman, A., Koudstaal, P.J., and Breteler, M.M.B. (2003). Silent brain infarcts and the risk of dementia and cognitive decline. *N. Engl. J. Med.* **348**, 1215–1222.
8. Woldendorp, K., Indja, B., Bannon, P.G., Fanning, J.P., Plunkett, B.T., and Grieve, S.M. (2021). Silent brain infarcts and early cognitive outcomes after transcatheter aortic valve implantation: a systematic review and meta-analysis. *Eur. Heart J.* **42**, 1004–1015.
9. NeuroVISION Investigators (2019). Perioperative covert stroke in patients undergoing non-cardiac surgery (NeuroVISION): a prospective cohort study. *Lancet* **394**, 1022–1029.
10. Kang, D.H., Hwang, Y.H., Kim, Y.S., Bae, G.Y., and Lee, S.J. (2013). Cognitive outcome and clinically silent thromboembolic events after coiling of asymptomatic unruptured intracranial aneurysms. *Neurosurgery* **72**, 638–645. discussion 645.
11. Srivatsan, A., Mohanty, A., Saleem, Y., Srinivasan, V.M., Wagner, K., Seeley, J., Burkhardt, J.K., Chen, S.R., Johnson, J.N., and Kan, P. (2021). Cognitive outcomes after unruptured intracranial aneurysm treatment with endovascular coiling. *J. Neurointerv. Surg.* **13**, 430–433.
12. Bonares, M.J., Egeto, P., de Oliveira Manoel, A.L., Vesely, K.A., Macdonald, R.L., and Schweizer, T.A. (2016). Unruptured intracranial aneurysm treatment effects on cognitive function: a meta-analysis. *J. Neurosurg.* **124**, 784–790.
13. Wagner, K., Srivatsan, A., Mohanty, A., Srinivasan, V.M., Saleem, Y., Chorian, J., James, R.F., Chen, S., Burkhardt, J.K., Johnson, J., and Kan, P. (2021). Cognitive outcomes after unruptured intracranial aneurysm treatment with flow diversion. *J. Neurosurg.* **134**, 33–38.
14. Lambin, P., Leijenaar, R.T.H., Deist, T.M., Peerlings, J., de Jong, E.E.C., van Timmeren, J., Sanduleanu, S., Larue, R.T.H.M., Even, A.J.G., Jochems, A., et al. (2017). Radiomics: the bridge between medical imaging and personalized medicine. *Nat. Rev. Clin. Oncol.* **14**, 749–762.
15. Smits, M. (2021). MRI biomarkers in neuro-oncology. *Nat. Rev. Neurol.* **17**, 486–500.
16. Bretzner, M., Bonkhoff, A.K., Schirmer, M.D., Hong, S., Dalca, A., Donahue, K., Giese, A.K., Etherton, M.R., Rist, P.M., Nardin, M., and Regenhart, R.W. (2022). Radiomics-Derived Brain Age Predicts Functional Outcome After Acute Ischemic Stroke. *Neurology* **100**, e822–e833.
17. Zhang, Y.Q., Liu, A.F., Man, F.Y., Zhang, Y.Y., Li, C., Liu, Y.E., Zhou, J., Zhang, A.P., Zhang, Y.D., Lv, J., and Jiang, W.J. (2022). MRI radiomic features-based machine learning approach to classify ischemic stroke onset time. *J. Neurol.* **269**, 350–360.
18. Wang, H., Sun, Y., Ge, Y., Wu, P.Y., Lin, J., Zhao, J., and Song, B. (2021). A Clinical-Radiomics Nomogram for Functional Outcome Predictions in Ischemic Stroke. *Neurol. Ther.* **10**, 819–832.
19. Liu, B., Meng, S., Cheng, J., Zeng, Y., Zhou, D., Deng, X., Kuang, L., Wu, X., Tang, L., Wang, H., et al. (2022). Diagnosis of Subcortical Ischemic Vascular Cognitive Impairment With No Dementia Using Radiomics of Cerebral Cortex and Subcortical Nuclei in High-Resolution T1-Weighted MR Imaging. *Front. Oncol.* **12**, 852726.
20. Nishi, H., Oishi, N., Ishii, A., Ono, I., Ogura, T., Sunohara, T., Chihara, H., Fukumitsu, R., Okawa, M., Yamana, N., et al. (2020). Deep Learning-Derived High-Level Neuroimaging Features Predict Clinical Outcomes for Large Vessel Occlusion. *Stroke* **51**, 1484–1492.
21. Yu, Y., Xie, Y., Thamm, T., Gong, E., Ouyang, J., Huang, C., Christensen, S., Marks, M.P., Lansberg, M.G., Albers, G.W., and Zaharchuk, G. (2020). Use of Deep Learning to Predict Final Ischemic Stroke Lesions From Initial Magnetic Resonance Imaging. *JAMA Netw. Open* **3**, e200772.
22. Kim, D.Y., Choi, K.H., Kim, J.H., Hong, J., Choi, S.M., Park, M.S., and Cho, K.H. (2023). Deep learning-based personalised outcome prediction after acute ischaemic stroke. *J. Neurol. Neurosurg. Psychiatry* **94**, 369–378.
23. Azeem, F., Durrani, R., Zerna, C., and Smith, E.E. (2020). Silent brain infarctions and cognition decline: systematic review and meta-analysis. *J. Neurol.* **267**, 502–512.
24. Conen, D., Rodondi, N., Müller, A., Beer, J.H., Ammann, P., Moschovitis, G., Auricchio, A., Hayoz, D., Kobza, R., Shah, D., et al. (2019). Relationships of Overt and Silent Brain Lesions With Cognitive Function in Patients With Atrial Fibrillation. *J. Am. Coll. Cardiol.* **73**, 989–999.
25. Auffret, V., Campelo-Parada, F., Regueiro, A., Del Trigo, M., Chiche, O., Chamandi, C., Allende, R., Cordoba-Soriano, J.G., Paradis, J.M., De Larochellière, R., et al. (2016). Serial Changes in Cognitive Function Following Transcatheter Aortic Valve Replacement. *J. Am. Coll. Cardiol.* **68**, 2129–2141.
26. Das, R.R., Seshadri, S., Beiser, A.S., Kelly-Hayes, M., Au, R., Himali, J.J., Kase, C.S., Benjamin, E.J., Polak, J.F., O'Donnell, C.J., et al. (2008). Prevalence and correlates of silent cerebral infarcts in the Framingham offspring study. *Stroke* **39**, 2929–2935.
27. Iosif, C., Lecomte, J.C., Pedrolo-Silveira, E., Mendes, G., Boncoeur Martel, M.P., Saleme, S., and Mounayer, C. (2018). Evaluation of ischemic lesion prevalence after endovascular treatment of intracranial aneurysms, as documented by 3-T diffusion-weighted imaging: a 2-year, single-center cohort study. *J. Neurosurg.* **128**, 982–991.

28. Pikis, S., Mantziaris, G., Mamalis, V., Barkas, K., Tsanis, A., Lyra, S., Karakoulas, K., Petrosyan, T., and Archontakis, E. (2020). Diffusion weighted image documented cerebral ischemia in the postprocedural period following pipeline embolization device with shield technology treatment of unruptured intracranial aneurysms: a prospective, single center study. *J. Neurointerv. Surg.* **12**, 407–411.
29. Jiang, L., Miao, Z., Chen, H., Geng, W., Yong, W., Chen, Y.C., Zhang, H., Duan, S., Yin, X., and Zhang, Z. (2023). Radiomics Analysis of Diffusion-Weighted Imaging and Long-Term Unfavorable Outcomes Risk for Acute Stroke. *Stroke* **54**, 488–498.
30. Bretzner, M., Bonkhoff, A.K., Schirmer, M.D., Hong, S., Dalca, A., Donahue, K., Giese, A.K., Etherton, M.R., Rist, P.M., Nardin, M., et al. (2023). Radiomics-Derived Brain Age Predicts Functional Outcome After Acute Ischemic Stroke. *Neurology* **100**, e822–e833.
31. Li, W., Wang, A., Ma, C., Wang, Y., Zhao, Y., Zhang, Y., Wang, K., Zhang, Y., Wang, Y., Yang, X., et al. (2023). Antiplatelet therapy adjustment improved the radiomic characteristics of acute silent cerebral infarction after stent-assisted coiling in patients with high on-treatment platelet reactivity: A prospective study. *Front. Neurosci.* **17**, 1068047.
32. Li, B., Tang, H., He, G., Jin, Z., He, Y., Huang, P., He, N., and Chen, S. (2023). Tai Chi enhances cognitive training effects on delaying cognitive decline in mild cognitive impairment. *Alzheimers Dement.* **19**, 136–149.
33. Li, B., Tang, H., He, G., Jin, Z., He, Y., Huang, P., He, N., and Chen, S. (2023). Tai Chi enhances cognitive training effects on delaying cognitive decline in mild cognitive impairment. *Alzheimers Dement.* **19**, 136–149.
34. Sun, L., Diao, X., Gang, X., Lv, Y., Zhao, X., Yang, S., Gao, Y., and Wang, G. (2020). Risk Factors for Cognitive Impairment in Patients with Type 2 Diabetes. *J. Diabetes Res.* **2020**, 4591938.
35. Huang, B., Sollee, J., Luo, Y.H., Reddy, A., Zhong, Z., Wu, J., Mammarapallil, J., Healey, T., Cheng, G., Azzoli, C., et al. (2022). Prediction of lung malignancy progression and survival with machine learning based on pre-treatment FDG-PET/CT. *EBioMedicine* **82**, 104127.

## STAR★METHODS

### KEY RESOURCES TABLE

REAGENT or RESOURCE	SOURCE	IDENTIFIER
R 4.30 (R Foundation for Statistical Computing, Vienna, Austria).	R Software	N/A
Python (version 3.61)	Python Software	N/A

### EXPERIMENTAL MODEL AND STUDY PARTICIPANT DETAILS

#### Ethical statement

The study protocol was approved by the Ethics Committee of Beijing Tiantan Hospital (KY-2019-025-02) in accordance with the Declaration of Helsinki, and all participants provided written informed consent.

#### Study population

This multicenter observational study was conducted in four centers in China from January 2016 to December 2021 and comprised a retrospective study for model development (training cohort) and retrospective and prospective validation studies. The training cohort comprised UIA patients in the Hospital 1 clinical database who developed NICIs as visualized on DWI after stent placement. For external validation, an independent retrospective cohort from Hospital 2 was enrolled. To assess the applicability of the model in clinical practice, a prospective observational study was conducted in patients recruited from Hospital 3 and Hospital 4.

#### Inclusion and exclusion criteria

UIA patients aged  $\geq 18$  years with normal cognitive function who were treated with stent placement and developed NICIs as identified on DWI performed within 1 week of the procedure were eligible for study inclusion.

The exclusion criteria were as follows: (1) MRI contraindications (pacemaker, ferromagnetic implant, foreign body, claustrophobia); (2) low-quality DWI images/image artifact; (3) patients with postoperative delirium; (4) UIA treatment with endovascular parent artery occlusion; (5) cerebral hemorrhagic procedure-related complications; (6) simultaneous treatment for other cerebrovascular diseases; (7) inability to complete cognitive assessments during follow-up; (8) pregnant or lactating; and (9) severe systemic diseases, such as liver disease, kidney disease, congestive heart failure, and cancer.

A total of 526 patients from the four centers met the criteria and were enrolled. A study flow diagram can be seen in [Figure 1](#), and the study design and workflow are presented in [Figure S8](#).

### METHOD DETAILS

#### Experimental design

This study aimed to develop a predictive model for cognitive dysfunction in patients with UIA after stent placement. The retrospective study served as the training cohort, and the validation of the model involved both retrospective and prospective approaches. The study design also included three main stages. (1) Model development using data from Hospital 1 (retrospective training cohort); (2) External validation using data from Hospital 2 (retrospective cohort); (3) Prospective validation to test the model's applicability in real-time clinical practice using data from Hospital 3 and Hospital 4.

#### Data collection and cognitive evaluation

Clinical data were collected from medical records and operative reports. Detailed clinical characteristics are available in the [Methods S1](#). Cognitive function was evaluated using the Chinese Mini-Mental State Examination (MMSE)<sup>33,34</sup> with scores corrected for educational attainment. Cognitive impairment was defined as an MMSE score  $\leq 26$ . Patients were divided into two groups based on their cognitive status at the one-year follow-up: cognitive dysfunction (CD) and non-cognitive dysfunction (non-CD) groups.

#### Image acquisition, segmentation, feature extraction, and selection

MRI scans were performed within one week of the stenting procedure. All patients underwent conventional brain MRI, which included DWI, and T1- and T2-weighted images in axial, coronal, and sagittal planes. Details regarding MRI scanning protocols and procedures for segmenting regions of interest (ROI) are provided in the [Methods S2](#) and [S3](#). Three major steps were followed for image analysis: (1) Image standardization; (2) Hand-crafted radiomics feature extraction; (3) Deep learning feature extraction.

All features were normalized using a Z score method. Specifics on radiomics and deep learning feature extraction are available in the [Methods S4](#) and [S5](#). Radiomic feature selection involved the use of the intraclass correlation coefficient, Mann-Whitney U test,

Spearman's rank correlation, and least absolute shrinkage and selection operator (LASSO) regression. In total, 1046 handcrafted and deep learning features were extracted from each ROI per patient.

## QUANTIFICATION AND STATISTICAL ANALYSIS

### Signature construction and assessment

#### *Clinical signature*

Clinical features were analyzed using t-test, Mann–Whitney U test, or chi-square test. Features with  $p < 0.05$  were retained for further analysis. Spearman's rank correlation was used to assess correlations between features, and features with a correlation coefficient of  $<0.9$  were retained. The selected features were used as input for logistic regression models to construct the clinical risk model.

#### *Radiomics signature*

Feature selection was performed using intraclass correlation coefficient, Mann–Whitney U test, and Spearman's rank correlation. LASSO regression was applied to reduce feature variance further. Multiple machine learning models, including logistic regression, SVM, KNN, Random Forest, ExtraTrees, XGBoost, LightGBM, and MLP, were evaluated. 5-fold cross-validation was used to identify the best-performing radiomics signature. Hyperparameters for the machine learning models were optimized using grid search methods.

#### *DTL signature*

Features were extracted using deep learning models, and the same feature selection and validation processes as above were applied. Prediction probabilities from the best fine-tuned deep learning model were used to construct the DTL signature.

#### *DLRN*

The DLRN was developed by combining the radiomics, DTL, and clinical signatures through logistic regression analysis.

### Model validation and visualization

#### *Heatmap visualization*

Heat maps were generated using gradient-weighted class activation mapping (Grad-CAM) to visualize the DTL signature and highlight areas relevant to classification.<sup>35</sup>

#### *Model validation*

All signatures were validated using both retrospective and prospective validation cohorts. Predictive performance was evaluated through receiver operating characteristic (ROC) curves. Calibration curves were used to assess discrimination ability. Model fit was tested using the Hosmer-Lemeshow test. Decision curve analysis was performed to evaluate the clinical utility of each model. Data analysis and presentation were performed using R 4.30 (R Foundation for Statistical Computing, Vienna, Austria) and Python (version 3.61).